

2 ml

X-592-73-334

PREPRINT

NASA TM X 70514

PLUMES IN THE MANTLE

(NASA-TM-X-70514) PLUMES IN THE MANTLE
(NASA) 27 p HC \$3.50 CSCL 08E

N74-10382

Unclas
63/13 22092

M. A. KHAN

NOVEMBER 1973



GODDARD SPACE FLIGHT CENTER
GREENBELT, MARYLAND

PLUMES IN THE MANTLE

M. A. Khan*
Geodynamics Program Division

November 1973

GODDARD SPACE FLIGHT CENTER
Greenbelt, Maryland

*On leave from University of Hawaii

PRECEDING PAGE BLANK NOT FILMED

PLUMES IN THE MANTLE

M. A. Khan
Geodynamics Program Division

ABSTRACT

Free air and isostatic gravity anomalies for the purposes of geophysical interpretation are presented. Evidence for the existence of hotspots in the mantle is reviewed. The proposed locations of these hotspots are not always associated with positive gravity anomalies. Theoretical analysis based on simplified flow models for the plumes indicates that unless the frictional viscosities are several orders of magnitude smaller than the present estimates of mantle viscosity or alternately, the vertical flows are reduced by about two orders of magnitude, the plume flow will generate implausibly high temperatures.

CONTENTS

	<u>Page</u>
GRAVITY ANOMALIES	1
Reference to Equilibrium Figure	1
Isostatic Gravity Anomalies	1
PLUMES IN THE MANTLE	6
DYNAMIC IMPLICATIONS OF MANTLE PLUMES	15
CONCLUSIONS	18

ILLUSTRATIONS

<u>Figure</u>		<u>Page</u>
1	Free Air Gravity Anamolies Based on GEM 4 Referred to $f = 1/298.255$	2
2	Free Air Gravity Anomalies Based on GEM 4 with Reference to the Equilibrium Figure	3
3	Isostatic Corrections in Milligals	4
4	Isostatic Gravity Anomalies Referred to the Equilibrium Figure	5
5	A Schematic Model of Plume Flow	7
6	Probable Locations of Hotspots (adapted from Morgan, 1972) . .	8
7	Relationship of Hotspot Locations with Isostatic Gravity Anomalies	9
8	Motion of Pacific Plate over Four Fixed Hotspots (after Morgan, 1972)	10
9	Location of Earthquakes and Recording Sites Used in Kanasewich et. al. (1972) Study (after Kanasewich et. al. 1972)	11
10	The $dT/d\Delta$ observations of initial P waves from all events between 20° and 100° recorded by VASA from June to August 1970. The $dT/d\Delta$ is obtained from the Jeffreys-Bullen tables for a normal depth source. Squares indicate events from Aleutians and Japan, triangles events from Tonga and Samoa; plus signs, events from South America; circles, events from Asia; crosses, special Solomon region events. Notice the time anomaly displayed by events from Tonga and Samoa for epicentral distances of 84° and 95° (after Kanasewich et. al. 1972).	12
11	Observations of phase velocity versus epicentral distances for Tonga earthquakes recorded by VASA. Triangles indicate events from Tonga-Samoa; plus signs, events from Asia, South America and Solomon Islands	13

ILLUSTRATIONS (Continued)

<u>Figure</u>		<u>Page</u>
12	Possible Core-Mantle Boundary Undulations in kms. ($n, m = 4, 4$) with Respect to Equilibrium Figure	14

TABLES

<u>Table</u>		<u>Page</u>
1	Typical Temperature Differences, Volume Flux and Density Differences for a Range of Flow Velocities	18

PLUMES IN THE MANTLE

GRAVITY ANOMALIES

Free air gravity anomalies based on a recent gravity model GEM 4 (Lerch et. al. 1972), derived from a combination of satellite and gravimetric data are shown in Figure 1. These anomalies are referred to a flattening of $f = 1/298.255$. For the use of these anomalies in geophysical interpretation two factors must be considered. First, the effect of departures from earth's hydrostatic state if the gravity anomalies are to be used in studying the stress distribution in the earth's interior. Second, the effect of surface topographic features if the anomalies are to be used for studying the subsurface mass distribution.

Reference to Equilibrium Figure

For studies of stress distribution, the gravity anomalies must be referred to a figure of zero stress. Such a figure is the equilibrium figure (Khan, 1969) i.e., the figure the earth would have assumed corresponding to its present rate of rotation if it were in a fluid state. Free air anomalies referred to this figure are shown in Figure 2. Its comparison with Figure 1 illustrates the importance of selecting the appropriate reference figure.

Isostatic Gravity Anomalies

The effect of topography is traditionally removed through isostatic correction. The classical methods of applying isostatic correction are laborious and time consuming. However, practically identical results can be achieved quickly by considering the surface topography and its compensation as surface densities (see, for example, Jeffreys, 1962; Khan, 1972). The potential due to isostatic reduction in this way is

$$U_{nm}^i = \frac{4\pi G}{2n+1} \sigma_{nm} S_{nm} \frac{R^{n+2}}{r^{n+1}} \cdot \left[1 - \left(\frac{R-d}{R} \right)^n \right]$$

where $\sigma_{nm} S_{nm}$ is the surface density layer, d the depth of compensation, n and m the degree and order respectively of the surface spherical harmonic S_{nm} and G the gravitational constant.

The isostatic corrections computed from the above equation are shown in Figure 3 (Khan, 1973). The consequent isostatic gravity anomalies are shown in Figure 4 (Khan, 1973). Notice that while the major features of the free air

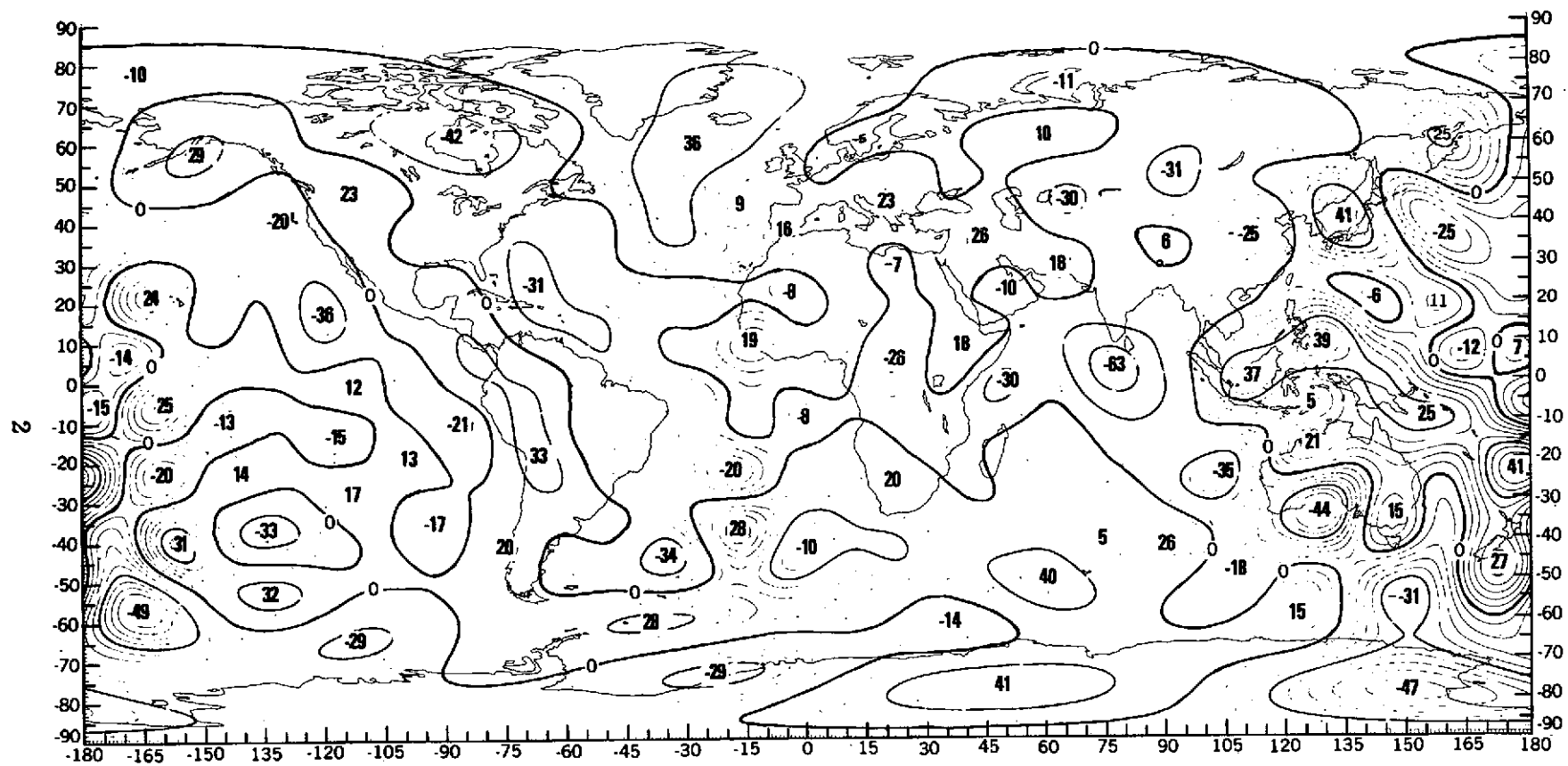


Figure 1. Free Air Gravity Anomalies Based on GEM 4 Referred to $f = 1/298.255$

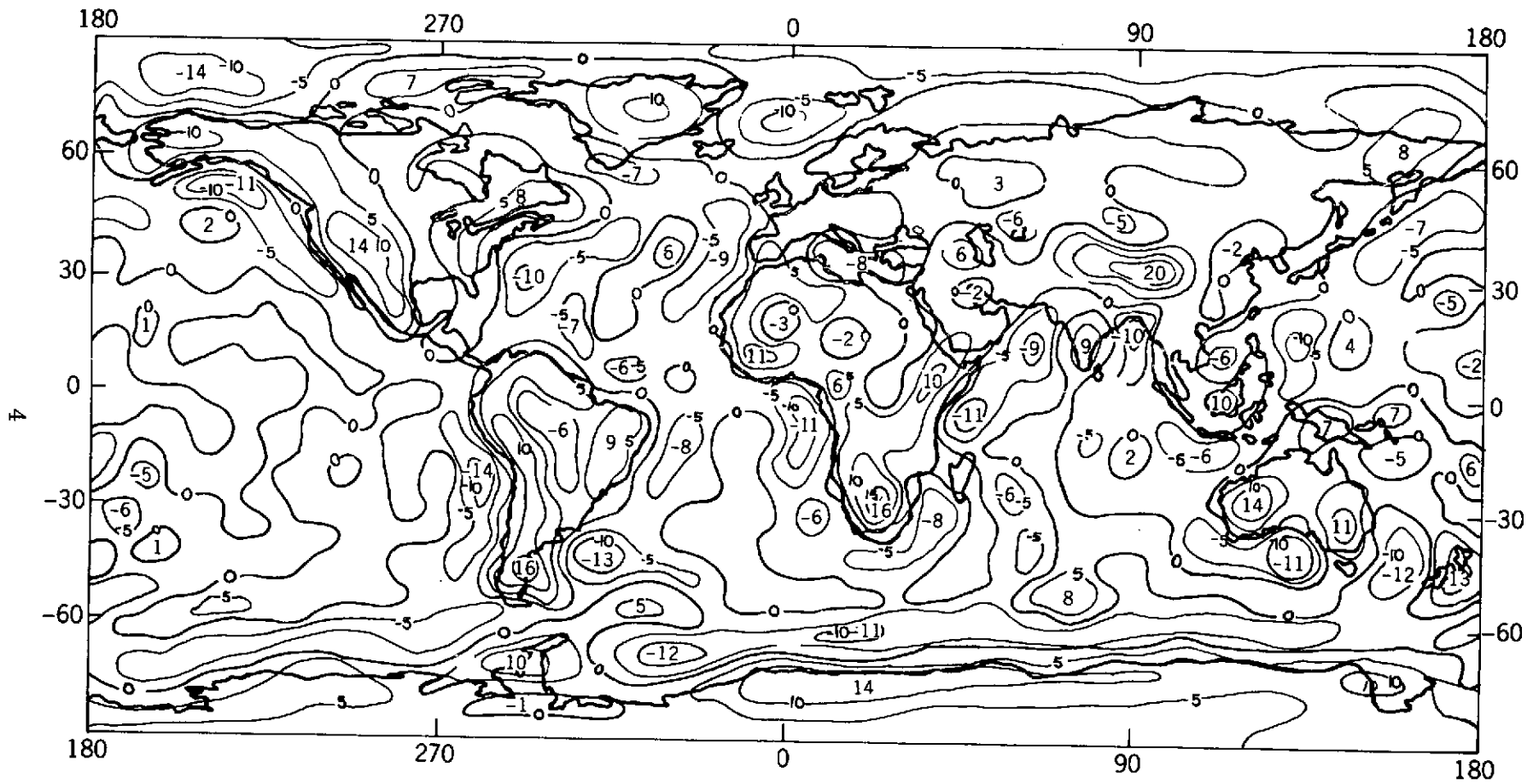


Figure 3. Isostatic Corrections in Milligals

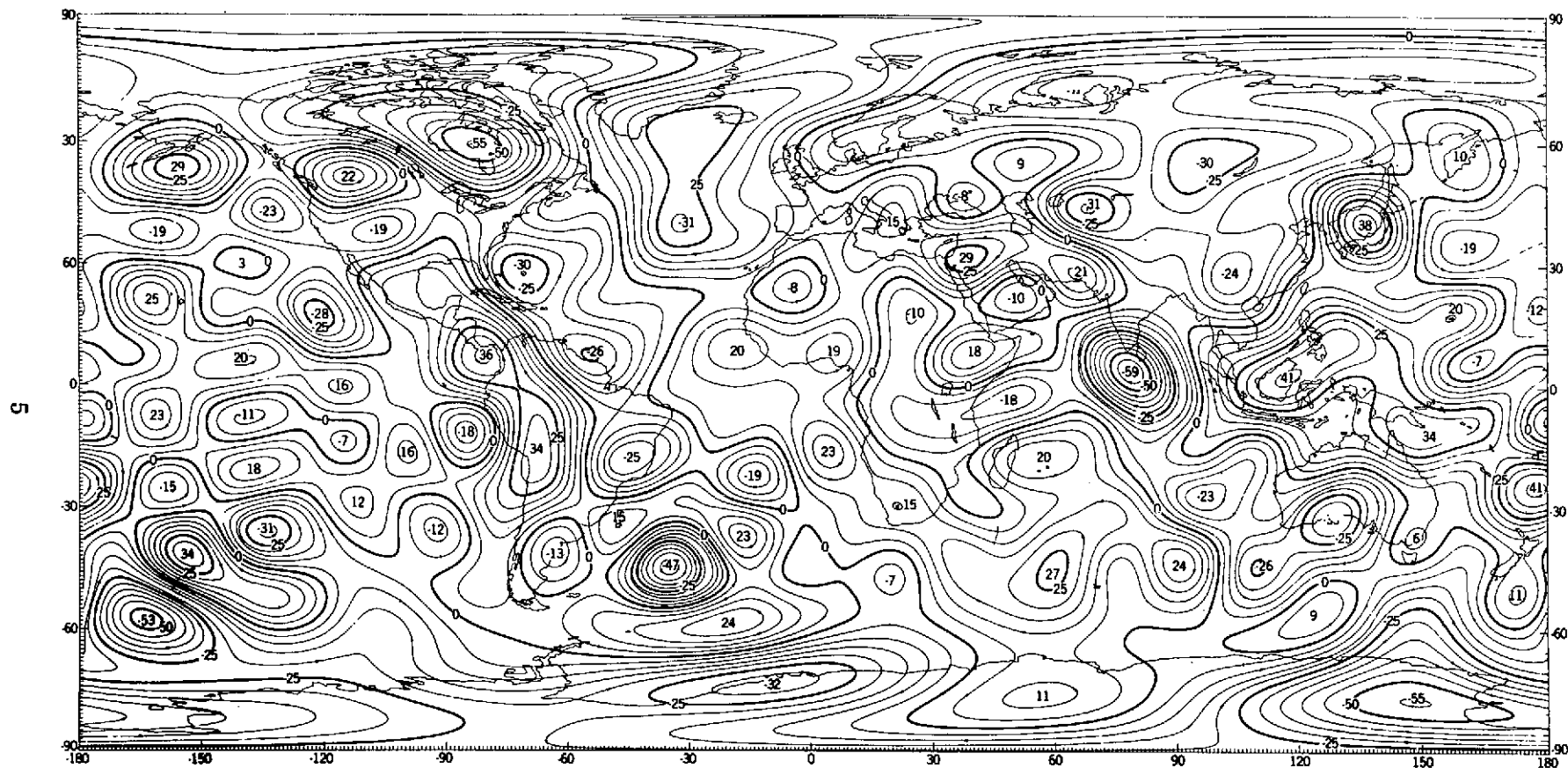


Figure 4. Isostatic Gravity Anomalies Referred to the Equilibrium Figure

gravity representation retain their identity (no dislocation occurs, only the amplitudes change) in the isostatic gravity representation, the gravity anomalies with relatively smaller amplitudes (<15 milligals) and shorter wavelength undergo a significant modification. For any global studies of the earth's interior, isostatic gravity anomalies are the most suitable representation.

PLUMES IN THE MANTLE

In this paper, we will not investigate the geotectonic significance of all the major features of the earth's gravity field. Instead, we will confine our analysis to certain aspects of the dynamic implications of recent idea of hotspots or mantle plumes using a simple rheological model for the mantle.

The idea of hotspots or mantle plumes was originally advanced by Wilson (1965) to explain the origin of island chains such as Hawaii and aseismic ridges such as Walvis Ridge. Morgan (1972) has related the idea to the motion of lithospheric plates. It is believed that hot, primordial material of deep mantle rises to the asthenosphere in narrow columns. To fill in the void created by the upwelling material, the rest of the mantle sinks slowly. In the asthenosphere the material coming through the plume spreads horizontally, flowing radially away from the upwelling source. The stresses caused by this radial flow on the bottom of the lithosphere plates have been suggested as a possible chief motivating force for driving the plate motion mechanism.

A schematic model of plume flow is shown in Figure 5. There are about twenty such plumes over the entire globe. Their proposed locations are shown in Figure 6. Major island chains and aseismic ridges are believed to be generated by the motion of rigid lithosphere plates over these hotspots which are believed to be more or less fixed relative to the mantle.

What geological and geophysical evidence is there to support such a hypothesis?

It is believed that the viscous drag exerted by the typical plume flow on the bottom of lithosphere will result in its doming, giving rise to a regional topographic high and an associated gravity excess over the area. Figure 7 shows the possible locations of these plumes superposed on the isostatic gravity anomalies. Most of these plumes are indeed in the general vicinity of gravity highs but there are several exceptions. A significant number of these plumes is also located in the zero gravity or negative gravity areas. See, for example, Galapos, Juan de Fuca, St. Helena, Macdonald and Salay Gomez.

Theoretical and experimental investigations seem to indicate that if convection does indeed exist in the lower mantle, very low Reynolds number of the mantle

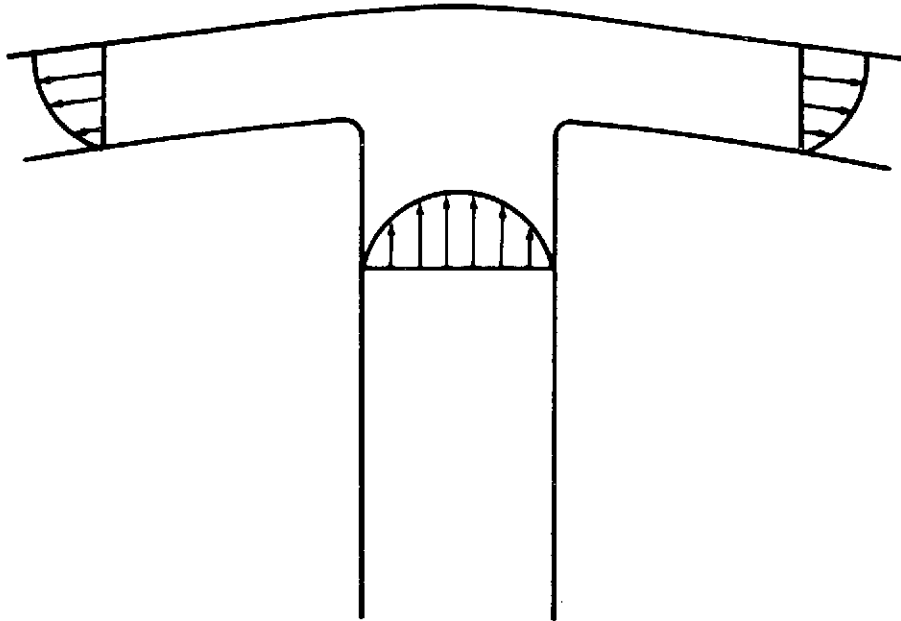


Figure 5. A Schematic Model of Plume Flow

will lead to flow patterns with minimum viscous dissipation and hence broad and smooth plumes (Kaula, 1972; Elsasser, 1971) while the temperature dependence of viscosity will make rising plumes much narrower than the sinking plumes (Torrance and Turcotte, 1971). On the other hand, the combined effect of heating from within and cooling at the surface will lead to rising plumes being much broader than the sinking plumes (Tozer, 1967) whereas high Prandtl number will lead to both rising and sinking flows being in narrow plumes (Turcotte and Oxburgh, 1967). Because of the complexity of convection theory and largely unknown properties of the mantle, it is uncertain how all these effects will combine to evolve a mantle flow system and what would be the characteristics of such a system. But theoretical evidence does indicate that, under certain conditions, the convective flow in the lower mantle, if it exists, would tend to localize in plume form.

Morgan (1972) has asserted that the movement of a rigid Pacific plate over four fixed hotspots can explain simultaneously the origin of Hawaiian Islands — Emperor Seamounts, Tuamotu Islands — Line Islands, Austral Islands — Gilbert-Marshall Islands, and the seamount chains in the Gulf of Alaska as shown in Figure 8. At the same time, the pattern of motion of the Pacific plate required to explain the origin of these island chains agrees with the paleomagnetic studies of seamounts (Francheteau et. al. 1970). Also, ages of Hawaiian lavas seem to fit this explanation. The Hawaiian ridge trends approximately northwest-southeast. Lava ages fall off progressively from northwest

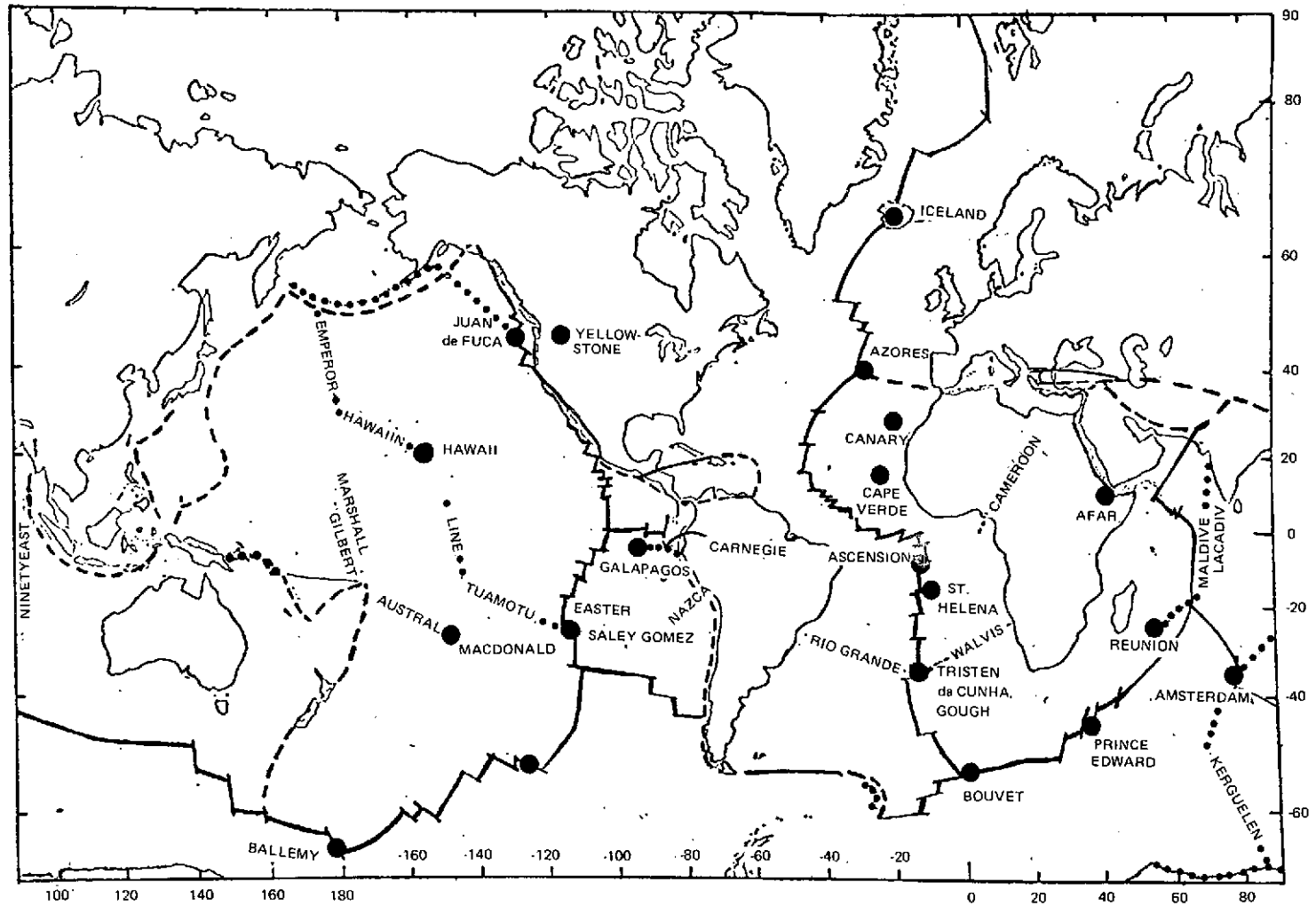


Figure 6. Probable Locations of Hotspots (adapted from Morgan, 1972)

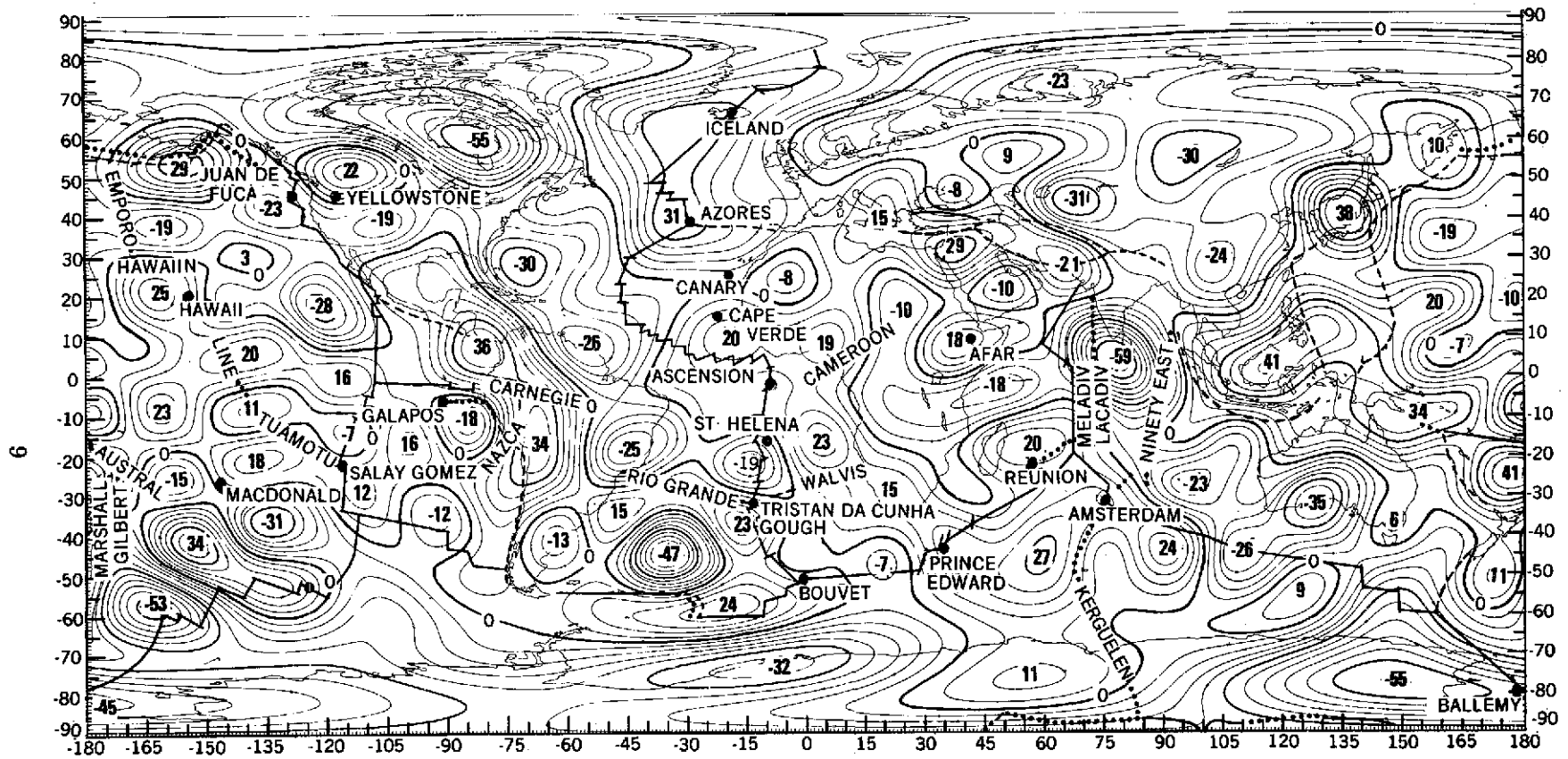


Figure 7. Relationship of Hotspot Locations with Isostatic Gravity Anomalies

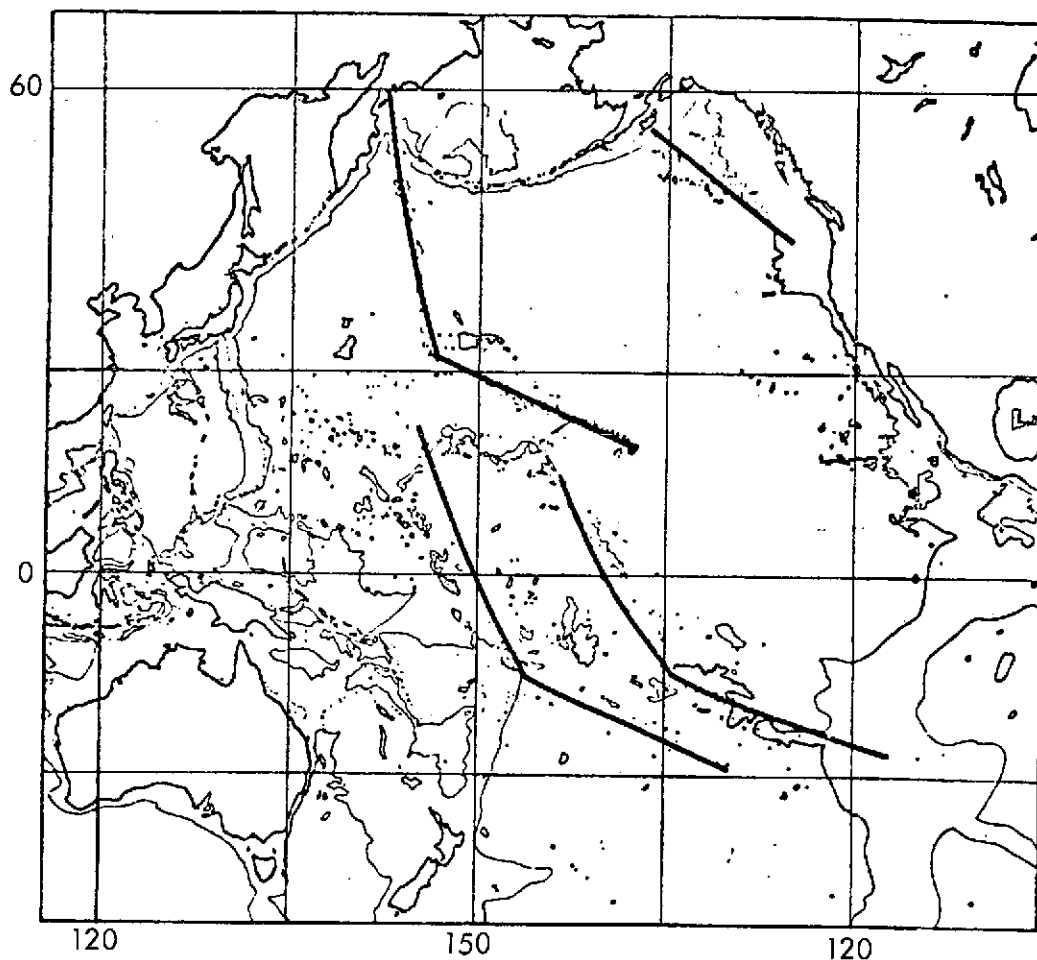


Figure 8. Motion of Pacific Plate over Four Fixed Hotspots (after Morgan, 1972)

to southeast extremity. Since the relative motion of Pacific plate is northwest, it would seem that the Hawaiian ridge is generated by the movement of the Pacific plate over a stationary lava source. A similar monotonically changing age relationship has been shown for Austral Chain (Wilson, 1965). Duncan et. al. (1972) contend that the origin of two igneous chains in the Continental European Plate — the Thulean volcanic province and the Central European volcanic province, also fits the "hotspots" idea provided appropriate polar wandering is allowed to reconcile the paleomagnetic results.

Kanasewich et. al. (1972) have reported that P arrivals recorded on an array in central Alberta from earthquakes in the vicinity of Tonga — Samoa Islands have anomalous values of phase velocity. Locations of earthquakes and recording sites used in their study are shown in Figure 9. The inverse of phase velocity,

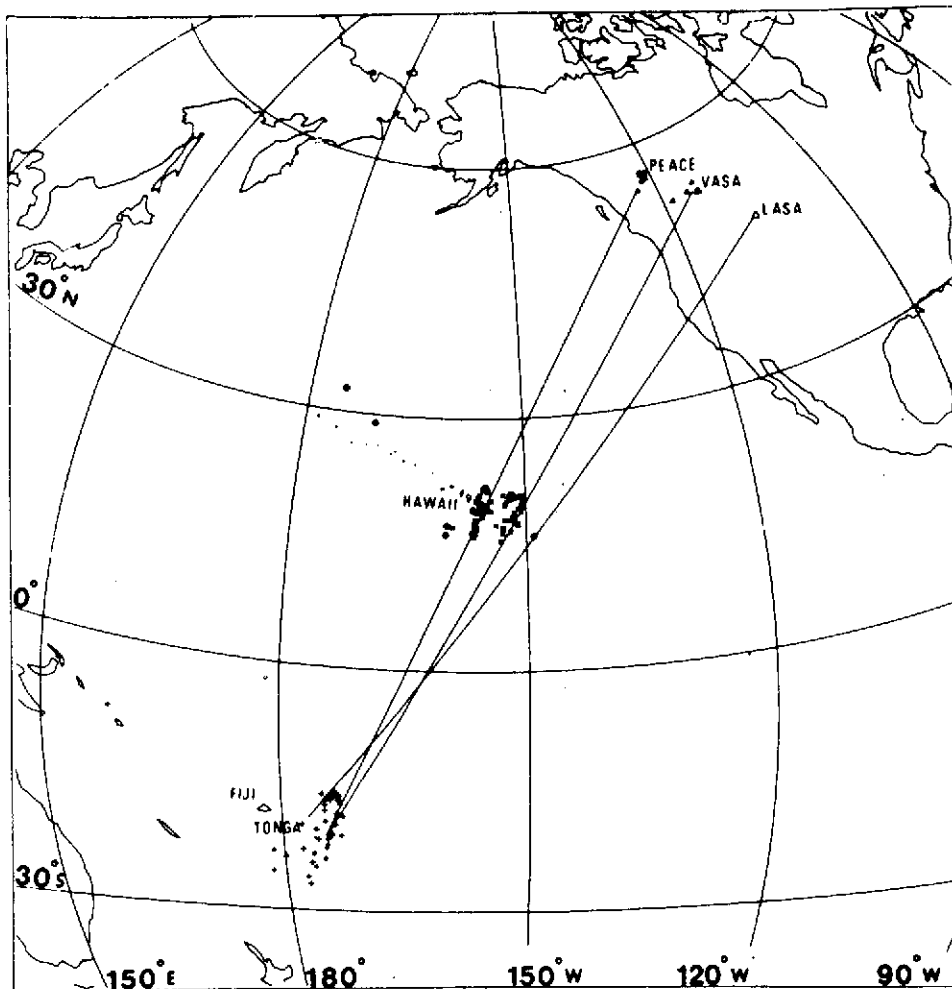


Figure 9. Location of Earthquakes and Recording Sites Used in Kanasewich et. al. (1972) Study (after Kanasewich et. al. 1972)

$dT/d\Delta$ and the phase velocities for these events are shown in Figures 10 and 11 respectively. It is clear from either Figure 10 or 11 that the phase velocity anomaly for Tonga — Samoa events increases from zero at epicentral distances of 84° to about 15% at epicentral distance of 95° when compared to normal phase velocities predicted from the Jeffreys-Bullen tables. The source of the phase velocity anomaly can be sought (a) at the source, (b) at the receiver, (c) at the turning point. Kanasewich et. al. (1972) argue that the anomaly could not originate in the hypocenter region as it would entail the existence of physically implausible lateral gradients. The anomalous source cannot be placed near the receivers as arrivals from the Pacific and Asia fall on the normal curve and rule out the required structural variation in the Moho. The source of the anomaly, therefore, must be placed at the turning point of the ray which falls beneath

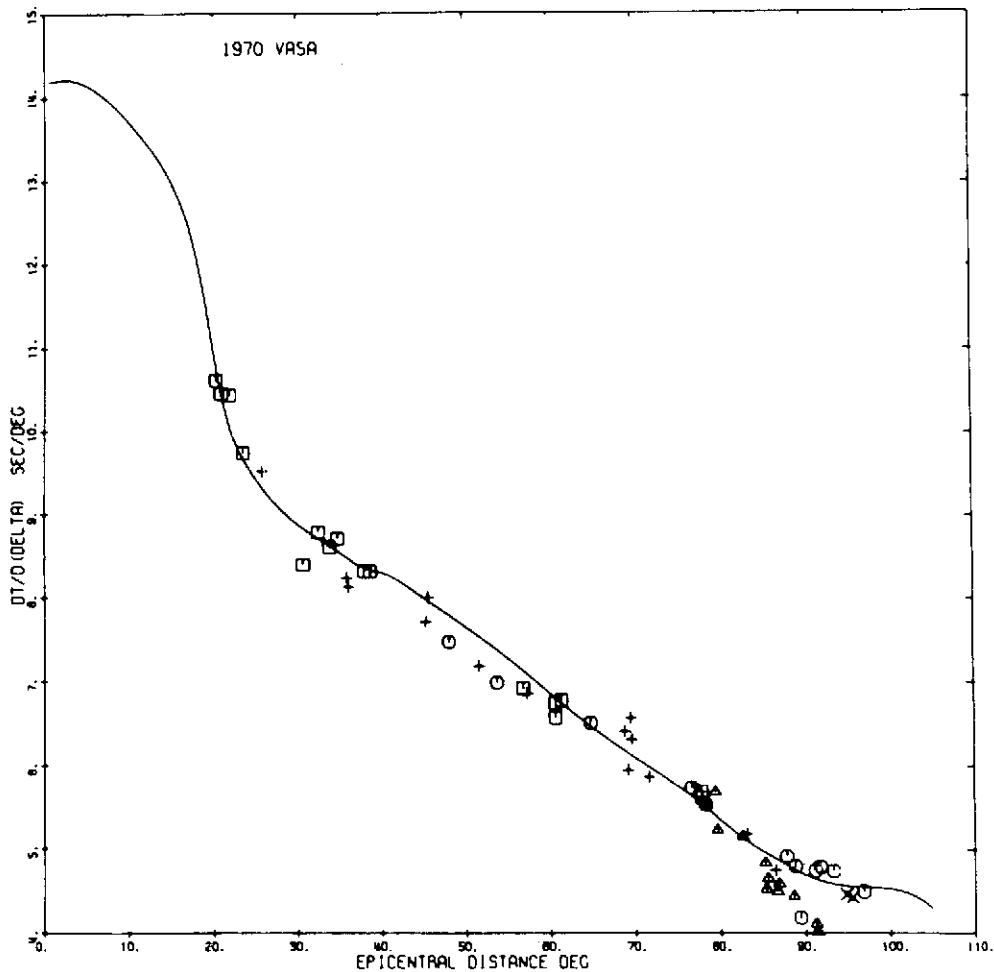


Figure 10. The $dT/d\Delta$ observations of initial P waves from all events between 20° and 100° recorded by VASA from June to August 1970. The $dT/d\Delta$ is obtained from the Jeffreys-Bullen tables for a normal depth source. Squares indicate events from Aleutians and Japan; triangles events from Tonga and Samoa; plus signs, events from South America; circles, events from Asia; crosses, special Solomon region events. Notice the time anomaly displayed by events from Tonga and Samoa for epicentral distances of 84° and 95° (after Kanasevich et. al. 1972).

Hawaii (Figure 9). The anomalous area seems to be about 10° in diameter, located below the southeast corner of the Hawaiian ridge. Normal events received into the PEACE array from the southern edge of Tonga define the western limit of this anomalous zone. Another normal event from Fiji into the LASA seems to define the eastern edge of this zone.

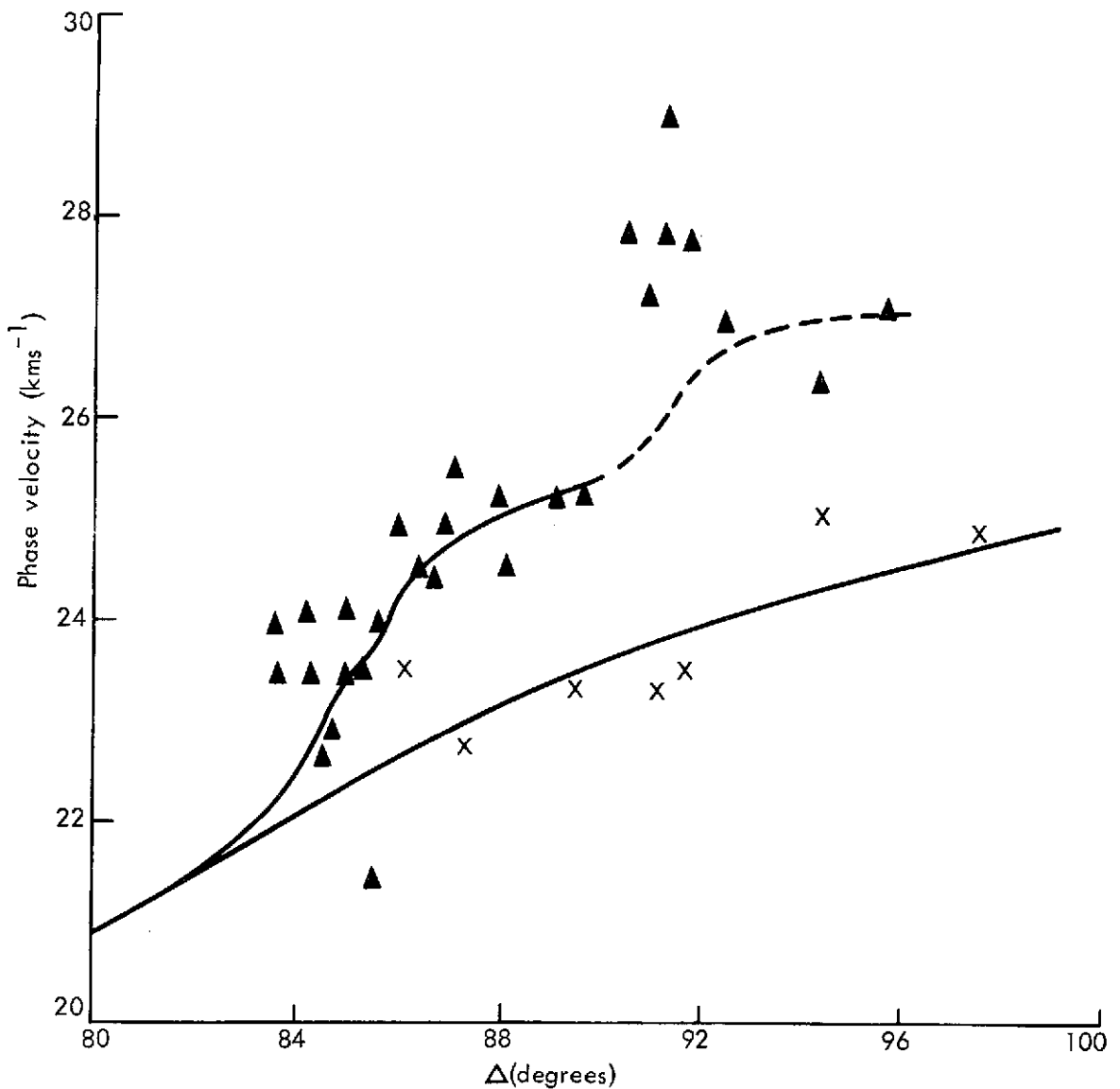


Figure 11. Observations of phase velocity versus epicentral distances for Tonga earthquakes recorded by VASA. Triangles indicate events from Tonga-Samoa; plus signs, events from Asia, South America and Solomon Islands.

The anomaly in phase velocity requires a depression of 125 kilometers on the core-mantle boundary. Observations of multiple reflections PnKP within the core as well as gravitational considerations (Buchbinder, 1972; Khan, 1971) rule out core-mantle boundary irregularities exceeding a few kilometers as illustrated in Figure 12 (based on gravitational considerations). Hence the phase velocity anomaly is interpreted by them (Kanasewich, et. al. 1972) as a radial and lateral

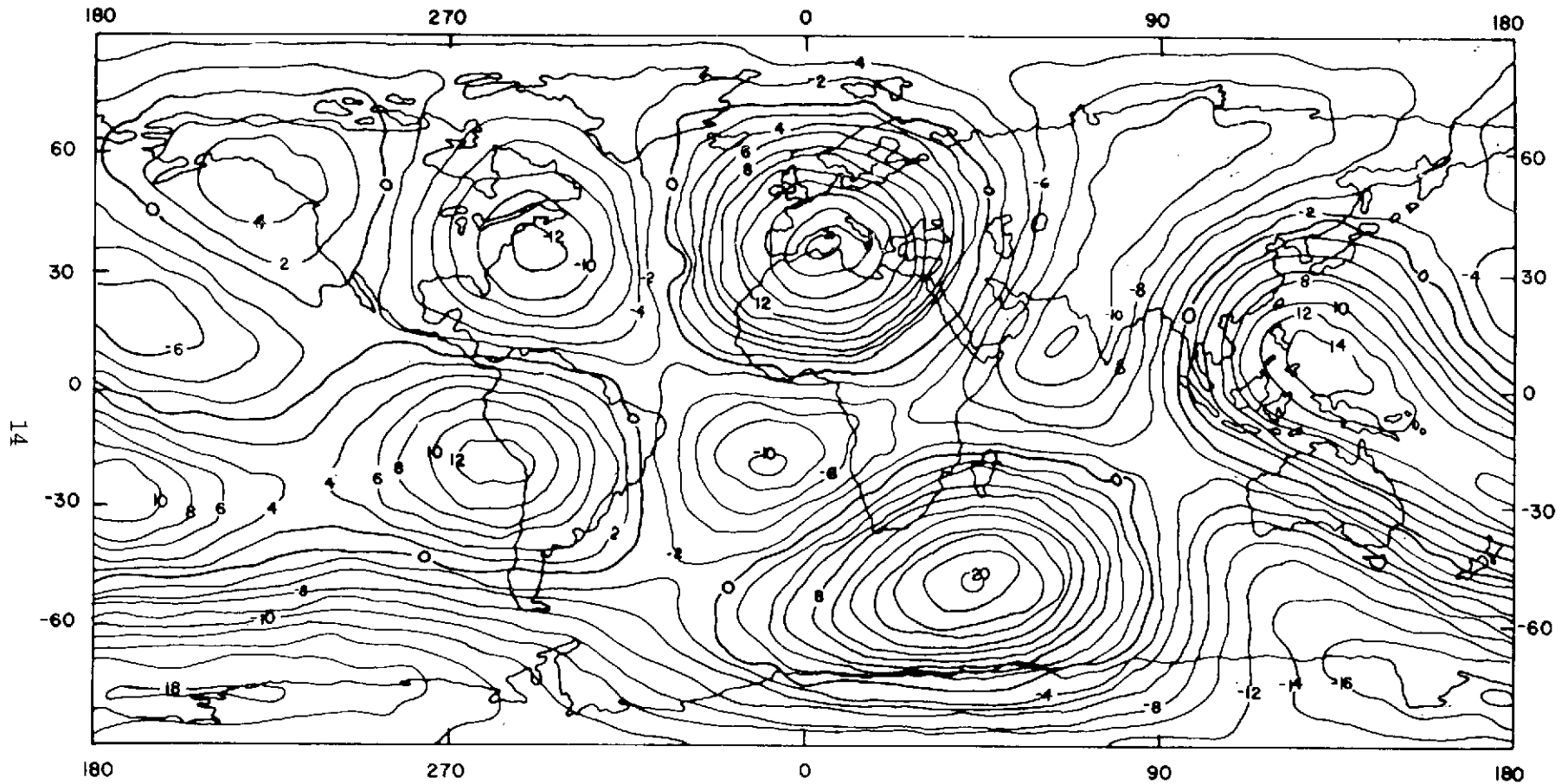


Figure 12. Possible Core-Mantle Boundary Undulations in kms. ($n, m = 4, 4$) with Respect to Equilibrium Figure

high velocity inhomogeneity in the lower mantle. Though the vertical extent of a possible inhomogeneity of this type is not clear, it has been interpreted as evidence for the existence of a mantle plume beneath Hawaii. Note however, that if this inhomogeneity is indeed the foot of a plume, it will be 1000 kms in diameter.

DYNAMIC IMPLICATIONS OF MANTLE PLUMES

Suppose the deep mantle material rising in the plume is of uniform viscosity. The Navier-Stokes equations of motion for a fluid of uniform viscosity are (Schlichting, 1960):

$$\rho \frac{d\mathbf{V}}{dt} = \rho \mathbf{F} - \nabla P + \frac{\eta}{3} \nabla (\nabla \cdot \mathbf{V}) + \eta \nabla^2 \mathbf{V}$$

where

\mathbf{F} = force per unit mass

ρ = density

∇P = pressure gradient

η = coefficient of viscosity

\mathbf{V} = velocity of flow

∇ = gradient.

If we now assume that (a) the fluid is incompressible, i.e., the divergence of the velocities is zero, and (b) the flow is steady state, i.e., the time dependent terms vanish, the Navier-Stokes equations reduce to

$$\rho \mathbf{F} - \nabla P + \eta \nabla^2 \mathbf{V} = 0$$

which are valid for Stokes flow types, i.e. flows with slow velocities and large distances.

Suppose the mantle plume flow is represented by highly viscous flow in a vertical pipe. Let a be the radius of the pipe so that at the center of the pipe $r = 0$ and at the walls $r = a$, and let z -axis be the axis of the pipe, then for the vertical flow we are considering, the Navier-Stokes equations in cylindrical coordinates reduce to form

$$\eta \left(\frac{d^2 V_z}{dr^2} + \frac{1}{r} \frac{dV_z}{dr} \right) = \frac{dp}{dz}$$

$$\frac{\partial p}{\partial r} = 0$$

For the boundary conditions $r = a, V_z = 0$; $r = 0, V_z = \text{max}$; and the conditions that V_z is a function of r only; p is independent of r and $\frac{dp}{dz} = \text{constant}$, the exact solution of above equations is

$$V_z = \frac{1}{4\eta} \frac{dp}{dz} (a^2 - r^2)$$

The maximum velocity occurs at $r = 0$, i.e.,

$$\text{Max } V_z = \frac{dp}{dz} \frac{a^2}{4\eta}$$

and the volume flux across the end of the pipe is

$$\text{volume flux} = \frac{dp}{dz} \frac{\pi a^4}{8\eta} = \frac{\pi a^2}{2} \cdot \text{Max } V_z$$

The associated energy equation in cylindrical coordinates in the general form (Schlichting, 1960) is

$$\rho \left(\frac{DE}{Dt} + p \frac{D(1/\rho)}{Dt} \right) = \frac{\partial Q}{\partial t} + \frac{1}{r} \frac{\partial}{\partial r} \left(rK \frac{\partial T}{\partial r} \right) + \frac{1}{r^2} \frac{\partial}{\partial \theta} \left(K \frac{\partial T}{\partial \theta} \right) + \frac{\partial}{\partial Z} \left(K \frac{\partial T}{\partial Z} \right) + \phi$$

where E = internal energy in unit mass considered

$\frac{\partial Q}{\partial t}$ = rate of heat produced per unit volume in the material

$$\frac{D}{Dt} = \frac{\partial}{\partial t} + V_r \cdot \frac{\partial}{\partial r} + V_\theta \cdot \frac{1}{r} \cdot \frac{\partial}{\partial \theta} + V_z \cdot \frac{\partial}{\partial Z}$$

ϕ = dissipation function depending upon η and strain components

and K = coefficient of heat conductivity

If we assume again, as in the case of Navier-Stokes equations, that (a) the flow is steady state, (b) fluid is incompressible, (c) viscosity coefficient is constant, (d) heat conductivity coefficient is constant, the energy equation reduces to

$$K \left(\frac{\partial^2 T}{\partial r^2} + \frac{1}{r} \frac{\partial T}{\partial r} + \frac{1}{r^2} \frac{\partial^2 T}{\partial \theta^2} + \frac{\partial^2 T}{\partial Z^2} \right) + \phi = 0$$

For the vertical flow we are considering the energy equation simplifies to

$$K \left(\frac{\partial^2 T}{\partial r^2} + \frac{1}{r} \frac{\partial T}{\partial r} \right) = \eta \left(\frac{\partial V_z}{\partial r} \right)^2$$

and with the boundary conditions $r = a$, $T = T_0$ and $r = 0$, $T = T_1$, we obtain the exact solution

$$T = T_0 + \frac{\eta \cdot \text{Max } V_z^2}{4K} \left(\frac{a^4 - r^4}{a^4} \right)$$

The maximum temperature T_1 is

$$T_1 = T_0 + \frac{\eta \cdot \text{Max } V_z^2}{4K}$$

so that maximum temperature change δT due to the flow is

$$\delta T = \frac{\eta \cdot \text{Max } V_z^2}{4K}$$

The temperature differences, volume flux and the density differences expected on the basis of the simplified model discussed above for a range of flow velocities are listed in Table 1. In these computations the typical values of $\eta = 3 \times 10^{21}$ gm cm⁻¹ sec⁻¹ and $K = 10^{-2}$ cal deg C⁻¹ cm⁻¹ sec⁻¹, the coefficient of thermal expansion $\alpha = 2 \times 10^{-5}$ deg C⁻¹, and density $\rho = 4$ gms/cm³ have been used. A typical plume is assumed to be roughly 150 kms in diameter.

Vertical velocities of plume flow are generally suggested to be 2m/year. Lower velocities will not bring enough material to the surface to make the hypothesis worthwhile in sea-floor spreading. However, as seen from Table 1, these velocities would generate implausibly high temperatures. If the velocities are scaled down to where the temperature differences become reasonable, the material brought up by the plumes is excessively small to account for sea-floor spreading. For example, for a velocity of 3 cm/year, the total material brought up by about 20 plumes will be merely 6 km³/year while from the known sea-floor spreading speeds, the rate is close to 170 km³/year.

Table 1.

Typical Temperature Differences, Volume Flux and Density Differences for a Range of Flow Velocities

Flow Velocity	Temperature Difference C°	Density Difference	Volume Flux per Plume
2 m/year	6.75×10^4	4 gm/cm ³	18 km ³ /yr.
1 m/year	1.69×10^4	1 gm/cm ³	9 km ³ /yr.
10 cm/year	1.69×10^2	10 ⁻² gm/cm ³	0.9 km ³ /yr.
3 cm/year	≈ 15°	10 ⁻³ gm/cm ³	2.7×10^{-1} km ³ /yr.
1 cm/year	≈ 2°	10 ⁻⁴ gm/cm ³	9×10^{-2} km ³ /yr.

This would mean that while asthenosphere currents, having a total flux of 6 km³/year are spreading away from the neighborhood of rise crests, opposing currents of the asthenosphere with a total flux of about 170 km³/year would be flowing towards the rises and the net stresses on the plates from this source would tend to close the lithospheric plates instead of moving them apart. This has been recognized by Morgan (1972) also. Hence for such low flow speeds, the hypothesis of plumes does not remain worthwhile in plate motion. The only alternative to scale down the temperature differences would be to reduce the viscosity by several orders of magnitude below the present estimates for it. The frictional viscosity will be sensitive to the temperature variations whereas we have made the assumption of constant viscosity in our model. It is possible that in the dynamics of plume flow in which the variation in viscosity arising from temperature variations is taken into account, the effects of increasing temperatures on viscosity and the effects of frictional viscosity to increase the temperatures, may balance in some way. It is not clear, however, that such considerations will reduce the frictional viscosity by the required orders of magnitudes to maintain reasonable thermal changes.

The temperature dependence of thermal conductivity will complicate the problem further. The extent of this effect is uncertain at this stage.

CONCLUSIONS

1. Free air and isostatic gravity anomalies are presented for use in geophysical interpretation.

2. Proposed locations of hotspots are generally in the vicinity of positive gravity anomalies, but several notable exceptions occur and the general claim that hotspots are associated with positive gravity cannot be supported.
3. Analysis of dynamic implications of plume flow based on simplified flow models indicates that such flows will generate implausibly high temperatures in the earth's interior unless the frictional viscosities are scaled down several orders of magnitude or alternately, the flow velocities are reduced by two orders of magnitude. But the frictional viscosity is the only real alternative as the reduction in flow velocities will make the hotspots hypothesis irrelevant to plate tectonics and consequently its invocation unnecessary. The frictional viscosity will indeed be sensitive to temperature variations — a factor not considered in this analysis, but whether temperature dependence of viscosity will reduce it by several orders of magnitude required to make the temperature variations reasonable is uncertain.

The temperature dependence of thermal conductivity will further complicate matters. The extent of this effect is uncertain.

REFERENCES

1. Buchbinder, G. G. R., Travel Times and Velocities in the Outer Core from PnKP, *Earth Planet. Sci. Letters*, 14, 161, 1972.
2. Duncan, R. A., N. Petersen and R. B. Hargraves, Mantle Plumes, Movement of the European Plate, and Polar Wandering, *Nature*, 239, 82-86, 1972.
3. Elsasser, W. M., Two layer Model of Upper Mantle Circulation, *J. Geophys. Res.*, 76, 4744-53, 1971.
4. Francheteau, J., C. G. Harrison, J. G. Sclater, and M. L. Richards, Magnetization of Pacific Seamounts, a Preliminary Polar Curve for the North-eastern Pacific, *J. Geophys. Res.*, 75, 2035-61, 1970.
5. Kanasewich, E. R., R. M. Ellis, C. H. Chapman and P. R. Gutowski, Teleseismic Array Evidence for Inhomogeneities in the Lower Mantle and the Origin of Hawaiian Islands, *Nature Physical Science*, 239, 99-100, 1972.
6. Kaula, W. M., Global Gravity and Mantle Convection, *Tectonophysics*, 13, 341-359, 1972.
7. Khan, M. A., General Solution of the Problem of Hydrostatic Equilibrium, *Geophys. J. R. Ast. Soc.* 18, 177-188, 1969.
8. Khan, M. A., Earth's Isostatic Gravity Anomaly Field, Goddard Space Flight Center No. X-592-73-199, 1973.
9. Khan, M. A., Some Geophysical Implications of the Satellite — Determined Geogravity Field, *Geophys. J.*, 23, 15-43, 1971.
10. Lerch, F., et. al., Gravitational Field Models GEM 3 and GEM 4, Goddard Space Flight Center No. X-592-72-476, 1972.
11. Morgan, W. J., Deep Mantle Convection Plumes and Plate Motions, *Am. Ass. Pet. Geologists Bull.*, 56, 203-213, 1972.
12. Schlichting, H., *Boundary Layer Theory*, McGraw-Hill Book Co., Inc., 1960.
13. Turcotte, D. L. and E. R. Oxburgh, Finite Amplitude Convection Cells and Continental Drift, *J. Fluid Mech.* 28, 29-42, 1967.
14. Torrance, K. E. and D. L. Turcotte, Structure of Convection Cells in the Mantle, *J. Geophys. Res.* 76, 1154-61, 1971.

15. Tozer, D. C., Towards a Theory of Thermal Convection in the Mantle, in the Earth's Mantle, ed. T. F. Gaskell, Academic Press, London, pp. 325-353, 1967.
16. Wilson, J. T., Evidence from Ocean Islands Suggesting Movements in the Earth, in Symposium on Continental Drift, Roy. Soc. London, Phil. Trans. Ser. A., 258, 145-167, 1965.